Applied Physics Letters

Enhanced optical Kerr nonlinearity of graphene/Si hybrid waveguide

Cite as: Appl. Phys. Lett. **114**, 071104 (2019); https://doi.org/10.1063/1.5064832
Submitted: 09 October 2018 . Accepted: 05 February 2019 . Published Online: 19 February 2019

Qi Feng, Hui Cong, Bin Zhang, Wenqi Wei, Yueyin Liang, Shaobo Fang, Ting Wang, and Jianjun Zhang

Applied Physics Letters ARTICLE scitation.org/journal/apl

Enhanced optical Kerr nonlinearity of graphene/Si hybrid waveguide

Cite as: Appl. Phys. Lett. **114**, 071104 (2019); doi: 10.1063/1.5064832
Submitted: 9 October 2018 · Accepted: 5 February 2019 ·
Published Online: 19 February 2019

View Online Export Citation CrossMark

Qi Feng,[1] Hui Cong,[1] Bin Zhang,[1,2] Wenqi Wei,[1,2,3] Yueyin Liang,[1,2] Shaobo Fang,[1,2] Ting Wang,[1,a)] and Jianjun Zhang[1,b)]

AFFILIATIONS

[1]Institute of Physics, Chinese Academy of Sciences, Beijing 100190, People's Republic of China
[2]School of Physical Sciences, University of Chinese Academy of Sciences, Beijing 100190, China
[3]School of Physics and Technology, Wuhan University, Wuhan 430072, China

[a)]Electronic mail: wangting@iphy.ac.cn
[b)]Electronic mail: jjzhang@iphy.ac.cn

ABSTRACT

In this work, we experimentally study the optical Kerr nonlinearities of graphene/Si hybrid waveguides with enhanced self-phase modulation. In the case of CMOS compatible materials for nonlinear optical signal processing, Si and silicon nitride waveguides have been extensively investigated over the past decade. However, Si waveguides exhibit strong two-photon absorption (TPA) at telecommunication wavelengths, which leads to a significant reduction of the nonlinear figure-of-merit (FOM). In contrast, a silicon nitride based material system usually suppresses the TPA but simultaneously leads to the reduction of Kerr nonlinearity by one order of magnitude. Here, we introduce a graphene/Si hybrid waveguide, which maintains the optical properties and CMOS compatibility of Si waveguides, while enhancing the Kerr nonlinearity, by transferring over to the top of the waveguides. The graphene/Si waveguides are measured to have an enhanced nonlinear parameter of 510 $W^{-1} m^{-1}$, compared with that of the Si waveguide of 150 $W^{-1} m^{-1}$. An enhanced nonlinear FOM of 2.48 ± 0.25 has been achieved, which is four times larger than that of the Si waveguide of 0.6 ± 0.1. This work reveals the potential application of graphene/Si hybrid waveguides with high Kerr nonlinearity and FOM for nonlinear all-optical signal processing.

Optical nonlinear effects in CMOS-compatible integrated optical devices are of great significance as they can be explored to realize a variety of functionalities ranging from all-optical signal processing to light generation.[1–5] A silicon-on-insulator (SOI) has been regarded as a popular platform for ultra-dense on-chip integration of photonic and electronic circuitry due to its compatibility with CMOS fabrication. In addition, the nonlinear optical properties of silicon waveguides are also heavily explored over the past decade, such as stimulated Raman scattering, Raman amplification, self-phase modulation (SPM), four-wave mixing, and super-continuum generation.[2,6–9] However, the existence of two-photon-absorption (TPA) at telecom wavelengths (around 1550 nm) in the Si platform leads to a strong degradation in the value of the nonlinear figure-of-merit (FOM). TPA increases the photon loss in the process and generates carriers subsequently producing usually undesired free-carrier absorption (FCA) and free-carrier dispersion (FCD). TPA and FCA generally cause optical losses, which in turn lower the peak power inside the waveguide and therefore reduce the conversion efficiency of the optical nonlinear process.[10,11] In addition, non-negligible single-photon absorption (SPA) should be taken into consideration not only at very low power levels but also at moderate powers.[12,13]

There are other promising platforms such as chalcogenide glass and AlGaAs, which possess high nonlinearity and low TPA, but highly challenging fabrication processes limit their usage in CMOS compatible applications.[14,15] Furthermore, CMOS compatible platforms such as Si_3N_4 and Hydex glass exhibit low TPA at telecom wavelengths, thus efficiently reducing the nonlinear loss as well as linear loss; however, their nonlinear refractive index is approximately one order of magnitude smaller than that of silicon.[16,17] Therefore, the best way to fulfill the requirement of silicon nonlinear photonics is to integrate them with materials with a high Kerr coefficient while keeping the silicon platform for its economic advantages.

One of the best candidates is graphene, which has outstanding optoelectronic properties, while remaining compatible for integration with silicon photonic devices. In the field of photonics, graphene has attracted widespread research attention in various optical devices, such as photodetectors, modulators, optical switches, optical gates, and lasers.[9,18–24] One of the major optical properties of graphene is the giant optical Kerr nonlinearity which has been previously reported by several groups with Kerr-coefficients ranging from 10^{-7} to 10^{-13} m^2/W.[25,26] The ultrahigh third order nonlinearity can facilitate grooming optically efficient nonlinear signal processing applications, which have been widely demonstrated, such as a slow-light graphene-Si photonic crystal waveguide, fiber pigtail cross-section coated with a single-layer graphene, and graphene-assisted Si microring resonator.[27–29] But the detailed optical nonlinear mechanism of graphene decorated Si waveguides as entire devices has not been experimentally investigated for CMOS compatible nonlinear silicon photonic applications. The understanding of graphene in a hybrid system leading to feasible optical switching devices can be of great use in future optoelectronic devices. In this paper, we demonstrate experimental studies of the SPM process under picosecond pulses in Si waveguides and graphene/Si (G/Si) hybrid waveguides. The positioning of graphene on Si waveguides was done by the transfer process. The effective Kerr coefficient n_2 of the graphene/Si hybrid waveguide is calculated to be $\sim 2 \times 10^{-17}$ m^2/W, which is three times larger than that of the Si waveguide. Furthermore, the FOM has been enhanced from 0.6 ± 0.1 in Si waveguides to 2.48 in G/Si hybrid waveguides.

Single-mode silicon waveguides with a width of 500 nm, a height of 340 nm, and a length of 3.5 mm are fabricated on a SOI wafer with a buried oxide layer of 3 μm. The schematic diagram of the waveguides is shown in Fig. 1(a). Standard e-beam lithography is used to pattern Si waveguides on a JEOL-6300 (100 kV) system with ZEP-520A EB resist. After development, the pattern is transferred by inductively coupled plasma (ICP) etching on Oxford PlasmaPro 100. The good quality of the sidewall is shown in Fig. 1(c). The inverse taper with a tip width of 100 nm and a tip length of 50 μm, as shown in Fig. 1(d), is designed to improve the efficiency of adiabatic coupling. Chemical vapor deposition (CVD)-grown monolayer graphene with a length of 60 μm is then transferred onto the waveguide and close to the input end by precise positioning.[30] Due to the absence of any folding or wrinkles of graphene under an optical microscope, we confirm that the graphene is totally flat on top of the silicon waveguides. The distance between the waveguide and the side silicon is 3 μm on both sides to avoid the mode leakage from the waveguide. It is noted that for comparison, identical silicon waveguides without graphene are fabricated using the same procedure.

The explicit characterization of monolayer graphene before and after transferring onto Si waveguides is carried out by Raman spectroscopic measurements, pumped with a 488 nm laser. As shown in Fig. 1(b), both the spectra show a G peak ($\sim$1586 cm^{-1}) with a full width at half maximum (FWHM) of $\sim$18 cm^{-1} and a 2D peak ($\sim$2700 cm^{-1}), with a 2D-to-G peak intensity ratio of about 1.2, implying the good quality of monolayer graphene.[31]

In order to investigate the third-order optical nonlinearity of G/Si hybrid waveguides, the dispersion and group velocity dispersion (GVD) are calculated using the standard Sellmeier equation by Lumerical MODE solutions. The group velocity dispersion as a function of wavelength for the silicon waveguide (denoted by the solid red line) and the G/Si hybrid waveguide (denoted by the dashed blue line) is presented in Fig. 2. The insets (a) and (b) in Fig. 1 show the electric field distribution of the TE mode in the silicon waveguide and the G/Si hybrid waveguide, respectively. The thickness of graphene in the simulation is set to be 1 nm, and the dispersive complex refractive index of graphene was used to calculate the dispersion curves for the

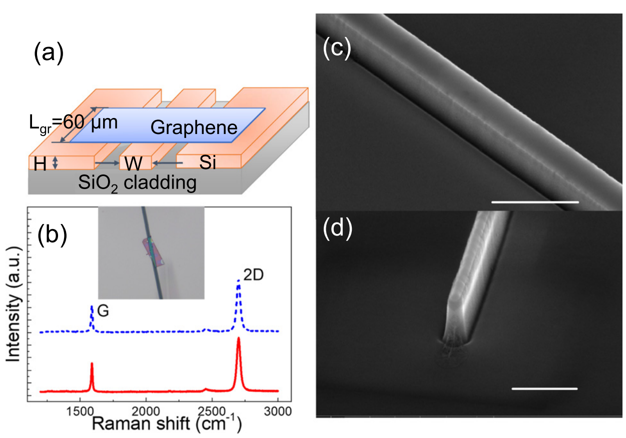

FIG. 1. (a) Schematic diagram of the graphene-Si hybrid waveguide, with the dimensions of W (500 nm) × H (340 nm) × L (3.5 mm). Raman spectra (b) of the single layer graphene before (red solid curve) and after (blue dotted curve) transferring onto the Si waveguide. Inset: optical microscopy image of graphene on the Si waveguide. Tilted SEM images of the (c) sidewall and (d) inverse taper of Si waveguides, with a scale bar of 1 μm and 500 nm, respectively.

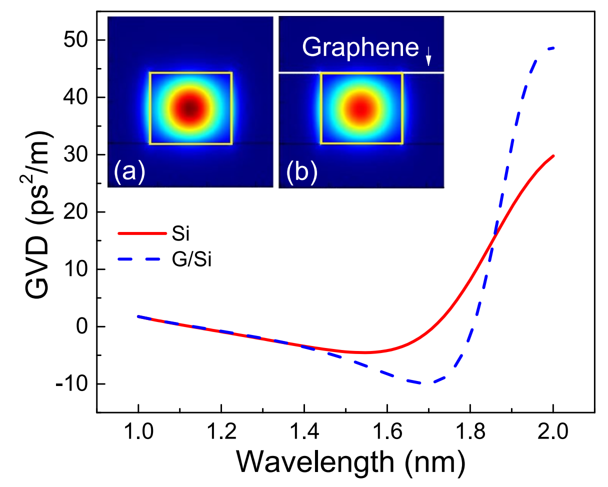

FIG. 2. Group velocity dispersion as a function of wavelength for silicon and G/Si hybrid waveguides, denoted by solid red and dashed blue curves, respectively. Inset: fundamental TE-mode optical intensity distribution of the (a) silicon waveguide and (b) G/Si hybrid waveguide. The graphene layer is indicated by a solid white line.

hybrid G/Si waveguides.[32] The group velocity dispersion is calculated to be $-4.5\ ps^2 m$ at 1550 nm. It is noted that compared with the GVD and dispersion of Si waveguides, the graphene in G/Si hybrid waveguides has a negligible effect on both GVD and dispersion.

Both Si and G/Si waveguides are pumped by a PriTel's FFL series of picosecond fiber lasers. The laser produces pulses with a center wavelength of around 1548 nm at a repetition rate of 20 MHz and a TE-mode pulse duration of 1.5 ps, which are delivered with a polarization-maintaining (PM) fiber and polarization controller. The transverse electric (TE) mode is chosen for the entire experiments because it supports the in-plane interaction between the evanescent field and the graphene, which is much stronger than the out-of-plane interaction due to the large optical anisotropy of two-dimensional materials.[9] The pulses are coupled into and out of the waveguide devices via lensed fibers and inverse taper with a coupling loss of approximately 10 dB per facet. It is noted that one meter long PM fiber between the pulse laser and the waveguide devices is chosen in order to eliminate the spectrum change induced from the nonlinear effects within the fiber. To monitor the input spectrum, a 90:10 coupler is inserted in the setup to split off 10% of the laser power into an optical spectrum analyzer (OSA, Yokogawa AQ6370D). The propagation loss measurements are carried out on Si waveguides by the cut-back method. The linear propagation losses in the silicon waveguide and those induced from graphene absorption are estimated to be (3.5 ± 0.5) dB/cm and 0.2 ± 0.02 dB/μm, respectively.

Prior to the SPM measurements, as shown in the insets of Fig. 3, we measure the temporal characteristics of the pulse by means of a frequency-resolved optical gating (FROG) instrument (Coherent Solutions HR150). A FROG scan records the spectrum of the nonlinear optical signal at each temporal delay. These data can be illustrated in the form of a so-called FROG trace. It contains both the temporal and spectral information about the pulse, as shown in the insets of Fig. 3. Note that because of the polarization sensitive nature of the FROG measurements, a short fiber length here was utilized to ensure that there was no significant depolarization during propagation. The pulse intensity and phase were characterized based on a spectrally resolved second harmonic generation (SG) autocorrelator. The Gaussian shape pulse of 1.5 ps has been confirmed as shown in the insets of Fig. 3. SPM measurements are carried out by measuring the transmission spectra in both Si waveguides and G/Si hybrid waveguides. It is shown in Fig. 3 that the dotted red curve represents the spectrum of the original input pulse, while the green and blue solid curves represent the output spectra for both the Si waveguide and the G/Si waveguide under identical input pulse energy, respectively. Of note, both waveguides have the same length of 3.5 mm. The input pulse has a spectral line-width of 2.1 nm. It shows the strong enhancement of third-order nonlinearity by integrating graphene with Si waveguides. The energy dependent measurements of the G/Si hybrid waveguide are shown in Fig. 4, with input pulse energies ranging from 5 pJ to 16 pJ. Since SPM alone is known to yield a symmetric spectral distribution around the injected laser frequency, the asymmetry must stem from other factors such as chirped injected laser pulses, self-steepening, GVD, or changes in the free carrier density by TPA. Self-steepening can be ruled out. First, the change of n_2 within the narrow spectral bandwidth of the ps-pulse is negligible. Second, the self-steepening induced spectral redshift is absent in our experiments.[33,34] GVD should be of minor influence, as will be discussed in detail later. Therefore, the FCA and TPA effects play a dominant role in this work.

Prior to the analysis of the nonlinear transmission, the relation between the average output power P_{out} and the average input power P_{in} is recalled in the case of a dominant TPA effect

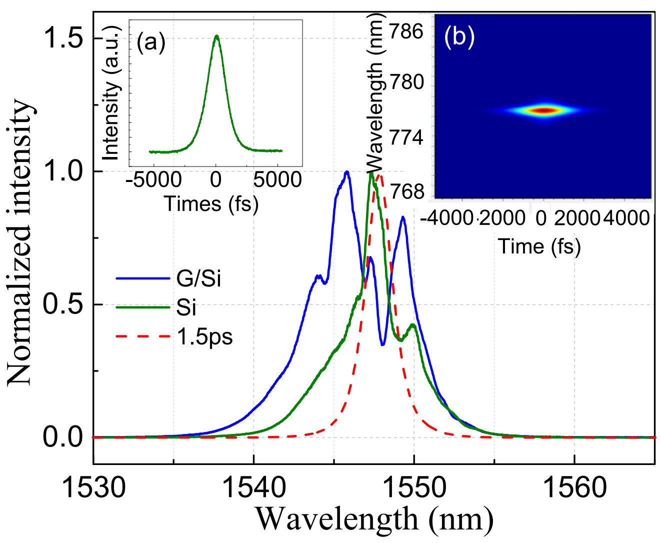

FIG. 3. Experimental results of the transmission spectra of comparison between the Si (green solid curve) and G/Si hybrid (blue solid curve) waveguides under the same input energy with 1.5 ps input pulse (spectrum denoted by the red dashed curve). Inset: (a) autocorrelation spectrum in the time domain and (b) second harmonic generation (SHG) FROG trace of a transform-limited Gaussian pulse with an FWHM of 1.5 ps.

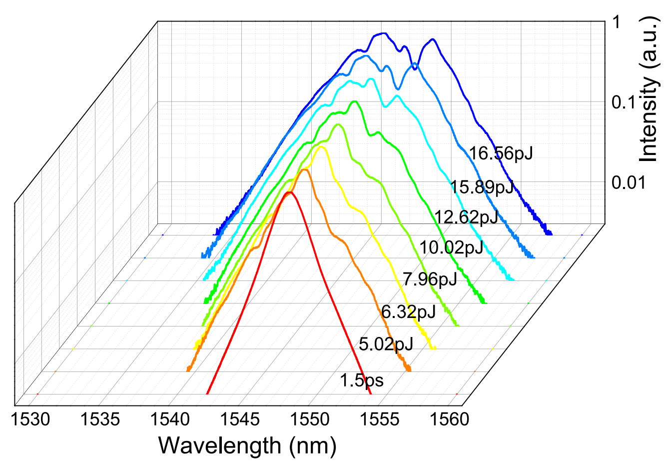

FIG. 4. The output spectra of the G/Si hybrid waveguide under various coupled energies. The red curve denotes the 1.5 ps pulse spectrum.

$$\frac{P_{in}}{P_{out}} = 2\mathrm{Im}(\gamma) L_{eff} e^{\alpha L} P_{in} + e^{\alpha L}, \tag{1}$$

where $\mathrm{Im}(\gamma) = \beta_{TPA}/(2A_{eff})$ is the imaginary part of the γ, nonlinear coefficient due to TPA, β_{TPA}, is the two-photon absorption coefficient, L_{eff} is the effective length reduced by the linear propagation loss through $L_{eff} = (1 - e^{-\alpha L})/\alpha$, L is the physical length, $\alpha = 3.5$ dB/cm is the linear propagation loss, and A_{eff} ($\sim$0.16 μm^2) is the effective mode area of waveguide. Thus, Eq. (1) discloses a linear relation between the ratio P_{in}/P_{out} and the measured input power P_{in} with the slope being proportional to the nonlinear coefficient β_{TPA}. The TPA coefficients β_{TPA} for both Si waveguides and G/Si hybrid waveguides can be extracted with similar values of 0.5 cm/GW.

We calculated the case where a Gaussian-shape laser pulse is coupled into the Si waveguide and G/Si hybrid waveguide. By using the nonlinear Schrödinger equation (NLSE) with the split-step Fourier method, the on-chip SPM process can be simulated with the following equation:[33]

$$\frac{\partial A}{\partial z} = -\frac{1}{2}\alpha A + i\sum_{m=2}^{10} \frac{i^m \beta_m}{m!}\frac{\partial^m A}{\partial \tau^m} + i\gamma |A|^2 A - \frac{\sigma}{2}(1 + i\mu) N_c A, \tag{2}$$

where A(z, t) is the slowly varying temporal envelope along the length z of a nonlinear medium, $\gamma = \omega_0 n_2 / cA_{eff}$ is the nonlinear parameter, ω_0 is the optical frequency, β_m is the m-th order dispersion coefficient, n_2 is the nonlinear Kerr coefficient, σ is the free carrier absorption coefficient, μ is the free carrier dispersion coefficient, and N_c is the free carrier density. N_c can be obtained by solving

$$\frac{\partial N_c}{\partial t} = \frac{\beta_{TPA}}{2\hbar\omega}\frac{|A|^4}{A_{eff}^2} - \frac{N_c}{\tau_c}, \tag{3}$$

where τ_c is the effective lifetime of free carriers with an estimated value of 0.5 ns.[10] Noting that pulse width $T_0 < \tau_c$, the τ_c term can be ignored as carriers do not have enough time to recombine over the pulse duration. The pulse dynamics are governed by the interplay of SPM and dispersion whose relative strengths can be determined by several characteristic lengths, namely, the GVD, defined as $L_D = T_0^2/|\beta_2|$, and the nonlinear length, defined as $L_{NL} = 1/\gamma P_{in}$.

Here, the nonlinear length L_{NL} and the dispersion length L_D, are calculated to be 0.65 mm and 19.26 mm, respectively. Given that L_D is much longer and L_{NL} is much shorter than the waveguide length (3.5 mm) for both Si and G/Si hybrid waveguides, the pulse dynamics will be dominated by the third-order nonlinearity rather than the dispersion.

As shown in Fig. 5, the simulated spectra have relatively good agreement with our experimental results under various input energies. The extracted n_2 value of the G/Si hybrid waveguide is here calculated to be 2×10^{-17} m^2/W, which is three times larger than that of the Si waveguide. Furthermore, the calculated nonlinear parameter γ is about 510 $W^{-1}m^{-1}$. In contrast, the calculated n_2 and nonlinear parameter γ of the Si waveguide are 6×10^{-18} m^2/W and 150 $W^{-1}m^{-1}$, respectively.

The nonlinear figure-of-merit can be defined as FOM $= n_2/(\lambda\beta_{TPA})$, which is a measure of the optical nonlinear efficiency of the medium when both the nonlinear refractive index and nonlinear loss mechanisms are accounted for.[35–37] In addition, it provides a useful dimensionless measurement of the suitability of the material for nonlinear switching. In this work, nonlinear FOM of the bare Si waveguide is $\sim 0.6 \pm 0.1$ at 1.55 μm, insufficient for optical switching applications, while the FOM of the G/Si hybrid waveguide is calculated to be approximately 2.48, which is higher than that reported in Si (0.83),[6] SiGe (0.26),[38] and hydrogenated amorphous-Si (0.66)[39,40] waveguides.

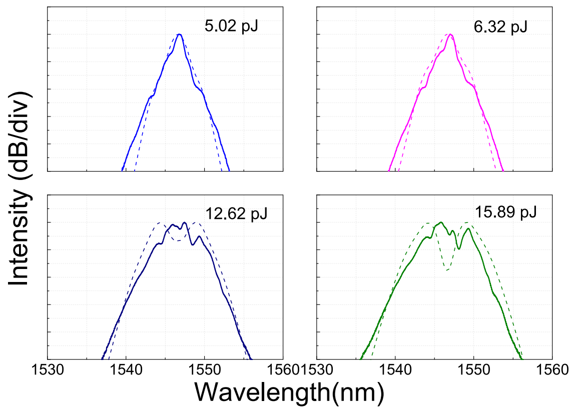

FIG. 5. Experimentally measured and numerically calculated spectra of the output picosecond pulse propagating along G/Si hybrid waveguides for various coupled pulse energies, denoted by solid and dashed curves, respectively.

In addition, for those platforms which possess low or negligible TPA in the telecom region, another figure of merit, $\gamma \times L_{eff,max}$, is more suitable. It provides a metric for comparison between nonlinear waveguides, where the acquired nonlinear phase scales linearly with the incident peak power. $L_{eff,max} = 1/\alpha$ is the maximum effective length achievable in a waveguide with a loss coefficient of α, and γ is the nonlinear parameter. The figures of merit $\gamma \times L_{eff,max}$ for Hydex glass[41] (loss = 0.06 dB cm^{-1} and $\gamma \sim 0.22\,W^{-1}m^{-1}$) and ultra-low-loss silicon nitride[42] (loss = 0.5 dB cm^{-1} and $\gamma \sim 1\,W^{-1}m^{-1}$) are calculated to be 0.16 and 0.087 W^{-1}, respectively. For the G/Si waveguides used in this work, $\gamma \times L_{eff,max} = 1.98\,W^{-1}$, which suggests that nonlinear waveguide devices implemented on this platform are able to achieve 10 times more nonlinear phase shift than ultra-low-loss platforms at the same peak power level. Furthermore, the field strength interaction between the silicon waveguide and graphene would be enhanced as the silicon waveguide changes to 220 nm in height due to the much higher electric field distribution, and this would further enhance the nonlinear behavior. The significant improvement in both the optical Kerr nonlinearity and nonlinear FOM in G/Si raises the prospect to provide a truly practical and viable platform for nonlinear photonic applications in the telecommunication wavelength window. This reveals that the incorporation of single layer graphene can be employed to increase the nonlinear performance of silicon-based waveguides in all-optical signal processing.

In summary, enhancement of third-order nonlinearity in the G/Si hybrid waveguide has been studied here by self-phase modulation experiments, and enhanced spectrum broadening has been observed in the G/Si hybrid waveguide. Although the decorated graphene exhibits a relatively weak evanescent fields in such a structure, three times larger Kerr nonlinearity is still achieved on the G/Si hybrid waveguide with an overall optical nonlinear parameter of 510 W^{-1}/m, higher than that of the silicon waveguide of 150 W^{-1}/m. The FOM has been improved as well from 0.6 ± 0.1 to 2.48 compared with that of the Si waveguide. The FOM for comparison with those platforms without TPA and G/Si hybrid waveguides is able to achieve 10 times more nonlinear phase at the same peak power level. This work provides an insight that on-chip integration of graphene with CMOS-compatible silicon platform enables the realization of devices that possess many all-optical functions at telecommunication wavelength.

The authors acknowledge the graphene transfer process by Dr. F. G. Yan from the Institute of Semiconductors, Chinese Academy of Sciences in China. Financial support was provided by the National Natural Science Foundation of China (Grant Nos. 11504415, 11434010, 11574356, 61635011, 11804382, and 61804177), the Ministry of Science and Technology (MOST) of People's Republic of China (2016YFA0300600 and 2016YFA0301700), and the Key Research Program of Frontier Sciences, CAS (Grant No. QYZDB-SSW-JSC009).

REFERENCES

[1]J. Leuthold, C. Koos, and W. Freude, Nat. Photonics **4**, 535–544 (2010).
[2]R. Claps, D. Dimitropoulos, V. Raghunathan, Y. Han, and B. Jalali, Opt. Express **11**, 1731–1739 (2003).
[3]T. K. Liang and H. K. Tsang, IEEE J. Sel. Top. Quantum Electron. **10**, 1149–1153 (2004).
[4]H. Rong, A. Liu, R. Jones, O. Cohen, D. Hak, R. Nicolaescu, A. Fang, and M. Paniccia, Nature **433**, 292–294 (2005).
[5]M. A. Foster, A. C. Turner, J. E. Sharping, B. S. Schmidt, M. Lipson, and A. L. Gaeta, Nature **441**, 960–963 (2006).
[6]H. K. Tsang, C. S. Wong, T. K. Liang, I. E. Day, S. W. Roberts, A. Harpin, J. Drake, and M. Asghari, Appl. Phys. Lett. **80**, 416–418 (2002).
[7]R. L. Espinola, J. I. Dadap, R. M. Osgood, S. J. McNab, and Y. A. Vlasov, Opt. Express **13**, 4341–4349 (2005).
[8]L. H. Yin, Q. Lin, and G. P. Agrawal, Opt. Lett. **32**, 391–394 (2007).
[9]C. Donnelly and D. T. H. Tan, Opt. Express **22**, 22820 (2014).
[10]L. H. Yin and G. P. Agrawal, Opt. Lett. **32**, 2031–2034 (2007).
[11]Q. Lin, O. J. Painter, and G. P. Agrawal, Opt. Express **15**, 16604–16644 (2007).
[12]A. Gil-Molina, I. Aldaya, J. L. Pita, L. H. Gabrielli, H. L. Fragnito, and P. Dainese, Appl. Phys. Lett. **112**, 251104 (2018).
[13]I. Aldaya, A. Gil-Molina, J. L. Pita, L. H. Gabrielli, H. L. Fragnito, and P. Dainese, Optica **4**, 1219 (2017).
[14]H. Lin, Y. Song, Y. Huang, D. Kita, S. K. Wang, L. Li, J. Li, H. Zheng, Z. Luo, H. Wang, S. Novak, A. Yadav, C.-C. Huang, R.-J. Shiue, D. Englund, T. Gu, D. Hewak, K. Richardson, J. Kong, and J. Hu, Nat. Photonics **11**, 798–806 (2017).
[15]P. Apiratikul, J. J. Wathen, G. A. Porkolab, B. Wang, L. He, T. E. Murphy, and C. J. Richardson, Opt. Express **22**, 26814–26824 (2014).
[16]J. P. Epping, M. Hoekman, R. Mateman, A. Leinse, R. G. Heideman, A. van Rees, P. J. M. van der Slot, C. J. Lee, and K.-J. Boller, Opt. Express **23**, 642–648 (2015).
[17]D. J. Moss, R. morandotti, A. L. Gaeta, and M. Lipson, Nat. Photonics **7**, 597–607 (2013).
[18]M. Liu, X. Yin, E. Ulin-Avila, B. Geng, T. Zentgraf, L. Ju, F. Wang, and X. Zhang, Nature **474**, 64–67 (2011).
[19]F. Xia, T. Mueller, T. Lin, A. Valdes-Garcia, and P. Avouris, Nat. Nanotechnol. **4**, 839–843 (2009).
[20]F. Bonaccorso, Z. Sun, T. Hasan, and A. Ferrari, Nat. Photonics **4**, 611–622 (2010).
[21]Y. Long, Y. Wang, X. Hu, M. Ji, L. Shen, A. Wang, and J. Wang, Opt. Lett. **42**, 799–802 (2017).
[22]M. Ji, H. Cai, L. Deng, Y. Huang, Q. Huang, J. Xia, Z. Li, J. Yu, and Y. Wang, Opt. Express **23**, 18679–18685 (2015).
[23]Y. Yang, Z. Xu, X. Jiang, Y. He, X. Guo, Y. Zhang, C. Qiu, and Y. Su, Photonics Res. **6**, 965–970 (2018).
[24]A. Ishizawa, R. Kou, T. Goto, T. Tsuchizawa, N. Matsuda, K. Hitachi, T. Nishikawa, K. Yamada, T. Sogawa, and H. Gotoh, Sci. Rep. **7**, 45520 (2017).
[25]A. K. Geim and K. S. Novoselov, Nat. Mater. **6**, 183–191 (2007).
[26]E. Hendry, P. J. Hale, J. Moger, A. K. Savchenko, and S. A. Mikhailov, Phys. Rev. Lett. **105**, 097401 (2010).
[27]H. Zhou, G. Tingyi, J. F. McMillan, N. Petrone, A. van der Zande, J. C. Hone, Y. Mingbin, L. Guoqiang, D.-L. Kwong, G. Feng, S. Zhou, and C. W. Wong, Appl. Phys. Lett. **105**, 091111 (2014).
[28]X. Hu, M. Zeng, A. Wang, L. Zhu, L. Fu, and J. Wang, Opt. Express **23**, 26158–26167 (2015).
[29]X. Hu, Y. Long, M. Ji, A. Wang, L. Zhu, Z. Ruan, Y. Wang, and J. Wang, Opt. Express **24**, 7168–7177 (2016).
[30]F. Yan, L. Zhao, A. Patanè, P. Hu, X. Wei, W. Luo, D. Zhang, Q. Lv, Q. Feng, C. Shen, K. Chang, L. Eaves, and K. Wang, Nanotechnology **28**, 27LT01 (2017).
[31]H. Li, Y. Anugrah, S. J. Koester, and M. Li, Appl. Phys. Lett. **101**, 111110 (2012).
[32]M. Bruna and S. Borini, Appl. Phys. Lett. **94**, 031901 (2009).
[33]G. P. Agrawal, *Nonlinear Fiber Optics* (Academic, San Diego, 2001).
[34]E. Dulkeith, Y. A. Vlasov, X. Chen, N. C. Panoiu, and R. M. Osgood, Opt. Lett. **14**, 5524–5534 (2006).
[35]V. R. Almeida, C. A. Barrios, R. R. Panepucci, and M. Lipson, Nature **431**, 1081–1084 (2004).
[36]K. W. DeLong, K. B. Rochford, and G. I. Stegeman, Appl. Phys. Lett. **55**, 1823–1825 (1989).
[37]V. Mizrahi, K. W. DeLong, G. I. Stegeman, M. A. Saifi, and M. J. Andrejco, Opt. Lett. **14**, 1140–1142 (1989).
[38]S. Serna, V. Vakarin, J.-M. Ramirez, J. Frigerio, A. Ballabio, X. Le Roux, L. Vivien, G. Isella, E. Cassan, N. Dubreuil, and D. Marris-Morini, Sci. Rep. **7**, 14692 (2017).
[39]J. Safioui, F. Leo, B. Kuyken, S.-P. Gorza, S. K. Selvaraja, R. Baets, P. Emplit, G. Roelkens, and S. Massar, Opt. Express **22**, 3089–3097 (2014).
[40]K. Narayanan and S. F. Preble, Opt. Express **18**, 8998 (2010).
[41]L. Razzari, D. Duchesne, M. Ferrera, R. Morandotti, S. Chu, B. E. Little, and D. J. Moss, Nat. Photonics **4**, 41–45 (2010).
[42]J. S. Levy, A. Gondarenko, M. A. Foster, A. C. Turner-Foster, A. L. Gaeta, and M. Lipson, Nat. Photonics **4**, 37–40 (2010).